academicJournals

Vol. 8(19), pp. 2090-2098, 23 May, 2013
DOI: 10.5897/AJAR11.523
ISSN 1991-637X ©2013 Academic Journals
http://www.academicjournals.org/AJAR

African Journal of Agricultural Research

Full Length Research Paper

Validating remote sensing derived evapotranspiration with the soil and water assessment tool (SWAT) model: A case study in Zhelin Basin, China

Chongliang Sun, Dong Jiang*, Juanle Wang and Yunqiang Zhu

State Key Laboratory of Resources and Environmental Information System, Institute of Geographical Sciences and Natural Resources Research, Chinese Academy of Sciences, China.

Accepted 15 May, 2013

Evapotranspiration (ET) is a major component in the water and heat balance of terrestrial ecosystems as well as in the water, energy and carbon cycles on the Earth's surface. A growing number of studies have focused on the retrieval of ET from remote sensing (RS) data. However, the RS-derived ET results could not be validated by station-observed data directly for the difference of the scale. The objective of this study is to present an operational approach to validation of RS-derived ET under the support of a distributed hydrological model: soil and water assessment tool (SWAT). Five years (2000-2004) evapotranspiration data of Zhelin Basin, the study area, were prepared. RS-derived ET and other data (DEM, land-use data, soil data, etc) were processed together in SWAT to simulate the hydrological cycle. The output monthly runoff is compared with observed runoff data. The RS-derived ET was then validated based on the results of those comparison (R^2=0.8516, RMSE=26.0860, MBE=-8.6578). It indicated that the method presented in the paper was an operational and feasible way for validation of ET data from remote sensing retrieval.

Key words: Distributed hydrological model, evapotranspiration, remote sensing, soil and water assessment tool (SWAT).

INTRODUCTION

Evapotranspiration (ET), including the evaporation from soil surface and the vegetation transpiration, is a major component in the water and heat balance of terrestrial ecosystems as well as in the water, energy and carbon cycles on the Earth's surface (Drexler et al., 2004; Gao, 2008; Hussey and Odum, 1992; Parasuraman et al., 2007; Zhou and Zhou, 2009).

Various ET studies have been conducted especially in arid regions on the basis of meteorological data with several main methods, such as Penman-Monteith method, Priestley-Taylor method, and the Hargreaves method, etc. (Amatya et al., 1995; Garcia et al., 2004; Gavilán et al., 2006; Lopez-Urrea et al., 2006; Mohan, 1991; Zhang et al., 2008). For daily ET calculation, the Penman-Monteith method requires the daily meteorological data, including the maximum and the minimum air temperature, the relative humidity, the solar radiation and the wind speed, as the input. The Priestley-Taylor method also requires multiple climate parameters to estimate ET, while the Hargreaves equation requires air temperature data to estimate ET. Since 1980s, with the emergence and rapid development of distributed hydrological models, remote sensing (RS) based approaches have been regarded as the preferred

*Corresponding author. E-mail: jiangd@igsnrr.ac.cn. Tel: +86-10-64889433. Fax: +86-10-64855049.

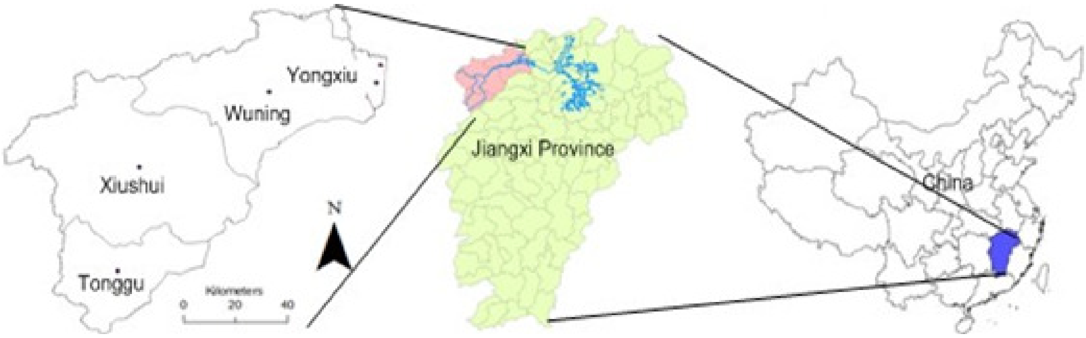

Figure 1. Location of the study area: Zhelin basin, Jiang Xi Province, China.

methods for estimating ET in large area with relative high spatial resolution (Overgaard et al., 2006). Numerous physical and empirical RS-based models have been developed for ET estimation in many different fields (Allen et al., 2005; Bastiaanssen, 2000; Bastiaanssen et al., 1998a, b; Granger, 1996, 2000; Jacob et al., 2002; Wang and Jiang, 2005). Most of RS methods for estimating ET are based wholly or partially on the energy balance principle, with net radiation adopted as the principal driving parameter (Jabloun and Sahli, 2008), which has led to a breakthrough in the high-resolution ET acquisition.

Unfortunately, problem exists in the validation of RS-derived ET data independently (Kite and Droogers, 2000). Since ET could not be observed directly, the ‘ground truth’ ET data were usually derived from Penman-Monteith method (etc.) using observed ET data, including the large aperture scintillomiter data (Jiang and Wang, 2003; Wang and Jiang, 2005) and the eddy covariance data (Boegh et al., 2009; Heilman et al., 2009; Kite and Droogers, 2000; Kustas and Norman, 1999; Sun and Song, 2008; Wu et al., 2006; Zhou and Zhou, 2009). The limitations are obvious for the in situ stations are rather limited in amount even in developed countries (Gavilán et al., 2006; Kite and Droogers, 2000), and the RS-derived ET could not be compared with station-observed data directly because the difference of the scale (Jabloun and Sahli, 2008; Liu et al., 2010). Additionally, the assumption that field methods are probably the most reliable is hard to justify, because different field methods differ considerably (Kite and Droogers, 2000).

Accordingly, proper method is urgently needed for validating the ET data obtained from RS retrieval. The objective of this study is to present an operational approach to validation of RS-derived ET under the support of a distributed hydrological model. The RS-derived ET, together with other auxillary data, were tansfered into runoff data by distributed hydrological model. The output runoff data could be compared with in situ observed runoff data, and then the ET could be validated accordingly. The soil and water assessment tool (SWAT) was adopted in this study. Among the advanced distributed hydrological models, SWAT has been widely used around the world, and some related researches on the calibration and sensitivity (Immerzeel and Droogers, 2008; Kannan et al., 2007a) as well as the climate change sensitivity have already existed (Ficklin et al., 2009). The method presented in this paper were tested and evaluated in the study area.

Study area

Zhelin Basin, the study area, is located in the upper and middle reaches of the Xiuhe River Basin in the Northeast Jiangxi province, China. It is one of the branches of the Yangtze River, with the Zhelin Reservoir in its lower reaches, which is located in east longitude 115.5 and north latitude 29.2°. The Zhelin Basin is in a strip shape, that is about 176 km from west to east and more than 84 km from south to north on average, with the altitudes within the range of 10 to 1200 m. The area of basin is about 9340 km^2, and the main river is about 353 km long with bending coefficient of 1.69. The basin is surrounded by mountains on three sides, that is, the Mufu Mountains in the north, the Dawei Mountains in the west and the Jiuling Mountains in the south. In this way, a closed watershed is formed. The land type composition of the basin is: 60% of mountains, 30% of hills, 7% of hillocks and the rest 3% of valley plains (Figure 1). The basin contains abundant ground vegetation, with dense forests full of firs and pines. Only in the middle reaches, scanty bald hills can be found, while sparse grassland is distributed in a few regions in the lower reaches.

The rainfall from April to June accounts for 50% of annual amount in Zhelin basin. In this area, the mean annual temperature is 16 to 17 DEG C, with the maximum temperature of about 29 DEG C emerging in July. The minimum mean monthly temperature of about 6 to 7 DEG C centers in January. The mean annual humidity is 80%, dispersing evenly in the whole area. The mean annual wind speed is at Grade 2.1; in terms of the spatial distribution, the value is lower in the upper

Table 1. The spatial resolution and purpose of the three spectra of GMS image.

Band's name	Visible band	Thermal infrared band	Vapour band
Spatial resolution(km)	1.25	5	5
Purpose	Evapotranspiration retrieval	Evapotranspiration retrieval	Validation

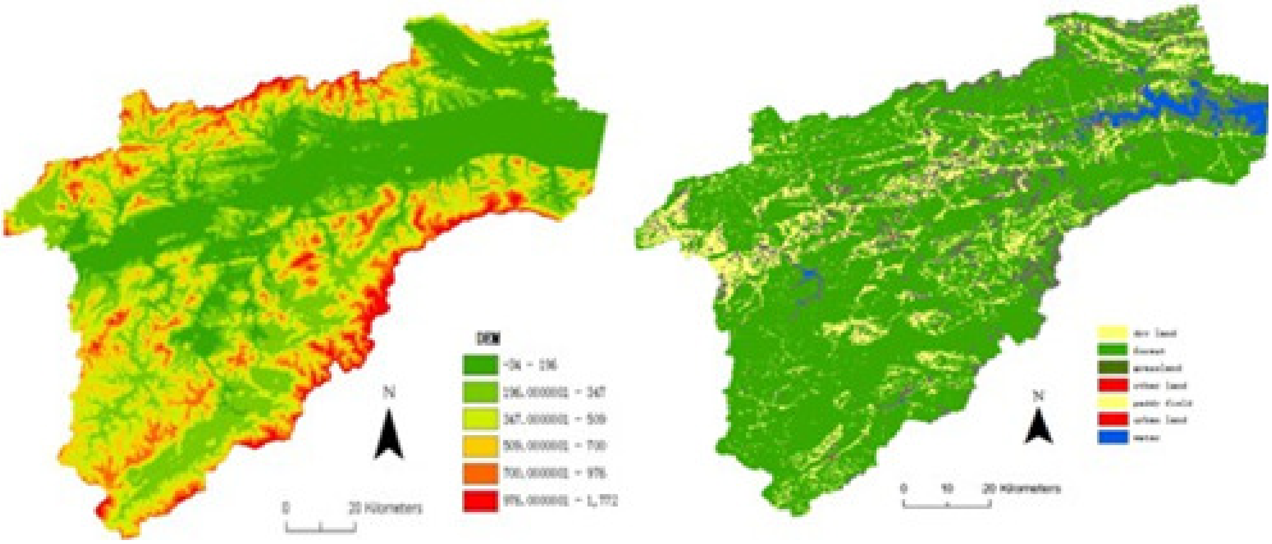

Figure 2. The DEM and land use of Zhelin basin.

reaches and higher in the lower reaches.

Data acquisition

RS data

Geostationary meteorological satellite data (GMS-5 data) were adopted as the data source for the ET retrieval. GMS-5 data can be easily acquired with relatively high temporal resolution (1 h). The GMS-5 data consists of three types of bands: (1) the visible band (VIS), with the spatial resolution of 1.25 km, and the spectrum range from 0.55 μm to 1.05 μm; (2) the thermal infrared band (TIR), with the spatial resolution of 5 km, and the spectrum range from 10.5 to 12.5 μm; (3) the water vapor band (WV), with the spatial resolution of 5 km, and the spectrum range from 6.2 to 7.6 μm. The visible and thermal infrared bands were employed for the ET retrieval, and the water vapor band was used for calibration and validation, as shown in Table 1.

Meteorological data

The meteorological data including daily precipitation, ET (obtained from retrieval), daily maximum temperature, daily minimum temperature, daily relative humidity, daily solar radiation and daily wind speed, were derived from National Resources and Environmental Database presented by Resources and Environmental Scientific Data Center (RESDC), Chinese Academy of Sciences.

DEM data

DEM data were used in the process of SWAT-based hydrological simulation. It was supplied by State Bureau of Surveying and Cartography (SBSC). The resolution of the DEM adopted in this study was 90 m, as shown in Figure 2.

Land use data

Land use data for 2005 were achieved from Landsat TM data through human-computer interactive interpretation, presented by Resources and Environmental Scientific Data Center (RESDC). Six land use types were identified including (1) cultivate land; (2) woodland; (3) grass land (4) water; (5) urban and rural settlements; (6) barren land. The scale of the land use map was 1:100,000. For the SWAT model, the attribute codes of the land use data were converted to the U.S. version, as shown in Figure 2.

Table 2. Datasets and their sources adopted in this study.

Data type	**DEM**	**Land use data**	**Property data**	**Soil data**
Sources	http://www.geodata.cn	http://www.geodata.cn and RESDC,CAS	thttp://www.geodata.cn and RESDC,CAS	http://www.geodata.cn
Usages	Input for SWAT	Input for SWAT; ET retrieval	Input for SWAT	Input for SWAT
Data type	Meteorological data	Runoff data	ET	GMS-5 RS data
Sources	The China meteorological administration; the information center of the Institute of Water Resources and Hydropower Research and the information center of Zhelin HydroPower Corp	the information center of the Institute of Water Resources and Hydropower Research and the information center of Zhelin HydroPower Corp	Retrieved in this study. And the ET should be processed into the data type and format as SWAT needed	http://satellite.cma.gov.cn/
Usages	Input for SWAT	Analysis for the simulated runoff	Input for SWAT	ET retrieval

All of the datasets are shown in Table 2 in details.

METHOD

ET retrieval model

A method based on the energy-balance theory developed by Wang and Jiang (2005) was adopted for ET retrieval. The RS-based latent heat flux was treated as the residual of the surface energy balance equation through model calculation (Boegh et al., 2002; Kustas et al., 1994; Moran et al., 1994). Accordingly, the energy balance equation can be expressed as:

$$LE = I_n - H - G - B \quad (1)$$

Where I_n is the net solar radiation flux, with W/m^2 as the unit; *H* is the sensible heat flux, with W/m^2 as the unit; *LE* is the latent heat flux, with W/m^2 as the unit; G is the soil heat flux, with W/m^2 as the unit; *B* is the energy absorbed by vegetation, with W/m^2 as the unit.

According to the above energy-balance principle, the following steps are required to retrieve ET from RS data: first, the surface albedo (*a*), the vegetation index (NDVI) and the surface temperature (T_0) should be acquired through a specific RS channel; then, I_n, H, G and B as well as the instantaneous evpotranspiration are calculated, and the daily ET is calculated based on LE_x.

$$I_n = (1-\alpha)I_g - L_\uparrow + L_\downarrow \quad (2)$$

Where Ig is the total solar radiation, a is the albedo, $L_\uparrow$is the long-wave radiation of the earth surface, and $L_\downarrow$ is the long-wave radiation of the atmosphere.

$$I_g = tS\cos(i_s) \quad (3)$$

Where S is the solar constant (W/m^2), t is the transmission coefficient of the atmospheric radiation, and i_s is the solar altitude angle.

$$L_\uparrow = \varepsilon_0 \sigma T_0^{\ 4} \quad (4)$$

$$L_\downarrow = \varepsilon_0 \varepsilon_a \sigma T_a^{\ 4} \quad (5)$$

Where T_0 is the surface temperature, Ta is the air temperature, ε_0 is the land surface emissivity, ε_a is the air emissivity, and σ is the Stefan-Boltzman constant.

According to the energy-balance principle, Brown and Rosenberg developed an impedance model for the sensible heat flux; Penmam-Monteith (Monteith, 1973) deduced a formula for H calculation:

$$H = -\rho C_p (T_a - T_0)/r_a \quad (6)$$

Where, T_0 is the ET surface temperature; T_a is the air temperature (at the attitude of 2.0 m); r_a is the surface roughness.

The heat flux G_0 （Z=0） of the surface soil can be calculated according to the following formula:

$$G_0 = R_n \cdot [\Gamma_c + (1-f_c)\cdot(\Gamma_s - \Gamma_c)] \quad (7)$$

Where, Γ_c is the canopy proportion coefficient; $\Gamma_s$is the bare-soil proportion coefficient; $f_c$is the vegetation coverage.

SWAT model

SWAT is a distributed hydrological model providing the spatial coverage of the integral hydrological cycle, including the atmosphere, plants, unsaturated zone, groundwater and surface water (Arnold et al., 1993; Neitsch et al., 2001). The model is comprehensively described in literatures (Arnold et al., 1998; Neitsch et al., 2002) and widely used around the world. According to the water-balance principle, the principle of SWAT can be described as:

$$SW_t = SW_0 + \sum_{i=1}^{t}(R_{day} - Q_{surf} - E_a - w_{seep} - Q_{gw}) \quad (8)$$

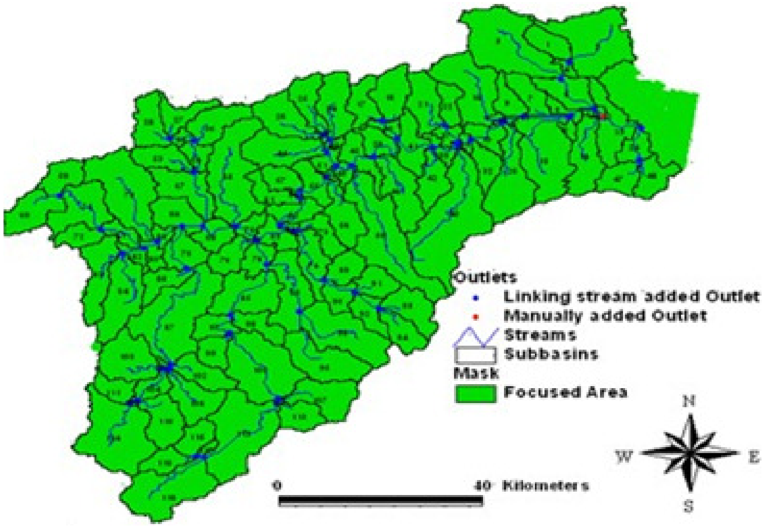

Figure 3. The map of the sub basin produced by SWAT.

Where, SW_t and SW_0 are the initial and the terminal water contents on day_i ; t is the time with a day as the unit; R_{day} is the rainfall on day_i ; Q_{surf} is the surface runoff on day_i ; E_a is the ET on day_i; w_{seep} is the infiltration amount; Q_{gw} is the runoff contribution from the groundwater .

Under SWAT, conceptually, the catchment is subdivided into sub basins and a river network based on DEM. SWAT integrates the simulation of weather, crop growth, ET, surface runoff, percolation, return flow, erosion, nutrient transport, groundwater flow, pond and reservoir storage, channel routing, field drainage, the water consumption of plants and other supporting processes . The tile drainage estimation is a function of the drain depth, the time needed for tile drains to bring the soil layer to field capacity and a drainage lag parameter. In SWAT, sub-catchments are divided into Hydrological Response Units (HRUs) as the unique combination of soil and land covers. The flow is not routed between HRUs, instead, the routing is used for flow in the channel network (Kannan et al., 2007b).

The input parameters of SWAT concern the ET studied in this paper, DEM, land use data, soil data, property data, the observed data for the outlet of the basin, meteorological data such as daily precipitation, daily maximum and minimum temperature, wind speed and relative humidity, as well as the runoff data on controlled sites and geographical materials, etc. The data required in SWAT for simulating the runoff and the data sources are shown Table 2.

The DEM of the catchment was prepared using the SRTM data with the spatial resolution of 90 m in the study area. Detailed land use information, which was acquired from RESDC and CAS, was used to draw the land use map and the soil map of the catchment. The Arc View-SWAT interface (AVSWAT-2000) was employed to delineate the catchment boundaries, and the burning-in option was used to acquire the drainage network. A visual inspection of the derived drainage network and the network delineation on the paper map showed good agreement. The multiple HRU options available in the AV-SWAT interface were applied with the objective of representing each field as a separate HRU. As a result, the study area was divided into 119 HRUs, as shown in Figure 3.

Validation of RS- derived ET

The study presented a new method of validating the remote-sensing retrieval of evapotranspiration under the support of the SWAT model. The RS-derived ET could not be evaluated by station-observed data directly because the difference of the scale. We suggested that the RS-derived ET could be evaluated by comparison of RS-computed Runoff (with SWAT) and the observed Runoff:

1. RS-derived ET is used as one of the input factors for SWAT,
2. RS-derived ET and other data (Digital Elevation Model (DEM), land use data , soil data, etc) are processed together in SWAT to simulate the hydrological cycle,
3. The Runoff is output from the SWAT,
4. Output Runoff is compared with observed runoff data,
5. RS-derived ET is evaluated based on the results of 4). Three indications, including the Root Mean Square Error (RMSE), the mean deviation error (MBE) and R^2, were employed for data analysis in this study.

The analysis flowchart are shown in Figure 4.

RESULTS AND ANALYSIS

Spatial-temporal variation of RS-derived ET

The monthly ET results from 2000 to 2004 in the Zhelin Basin obtained with RS retrieval method were analyzed. The whole Zhelin Basin involved 238 RS pixels. The daily and monthly ET results from 2000 to 2004 were shown in Figures 5 and 6.

The spatial distribution of the monthly ET was analyzed. In March, when the rainfall was relatively less throughout the whole year, the maximum ET emerged in the area with plenty of water, such as reservoirs and paddy fields, while the minimum ET appeared in the upper reaches of the basin and the area with high altitudes, as shown in Figure 5, which indicated that the primary factor affecting ET is the water capacity in this season. In June and September when the rainfall is

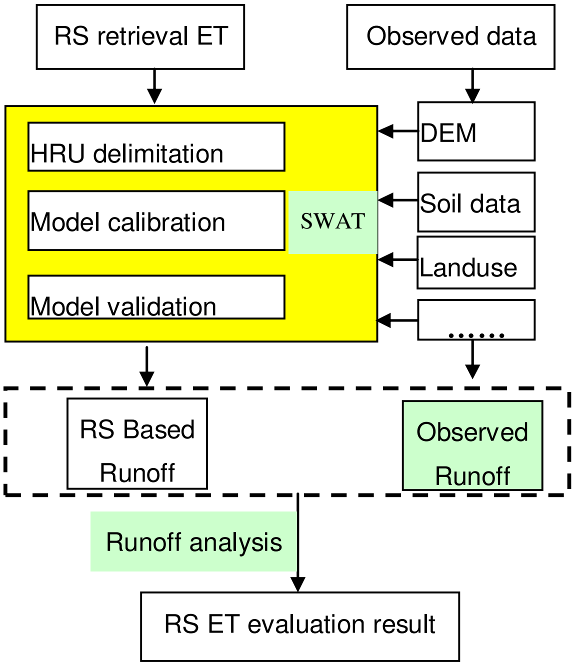

Figure 4. The flowchart of ET validation.

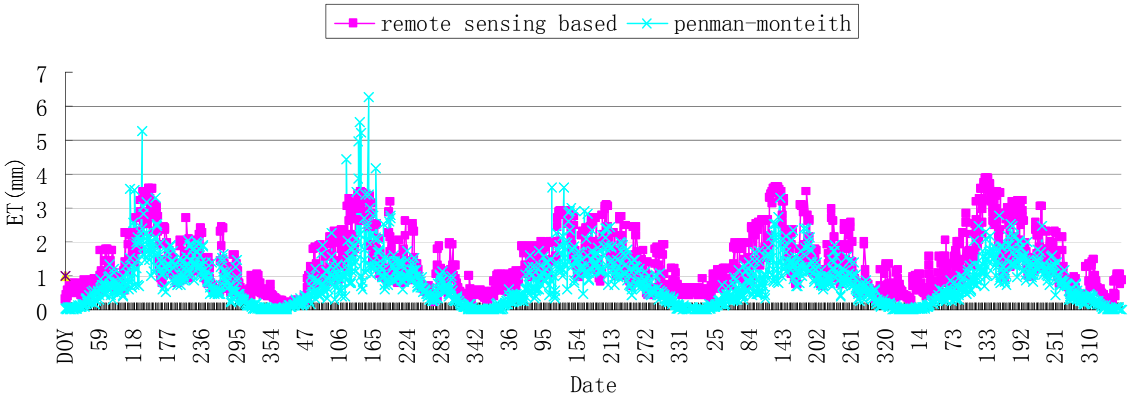

Figure 5. The daily ET result from the remote sensing based method and penman-monteithmethod from the year of 2000 to 2004.

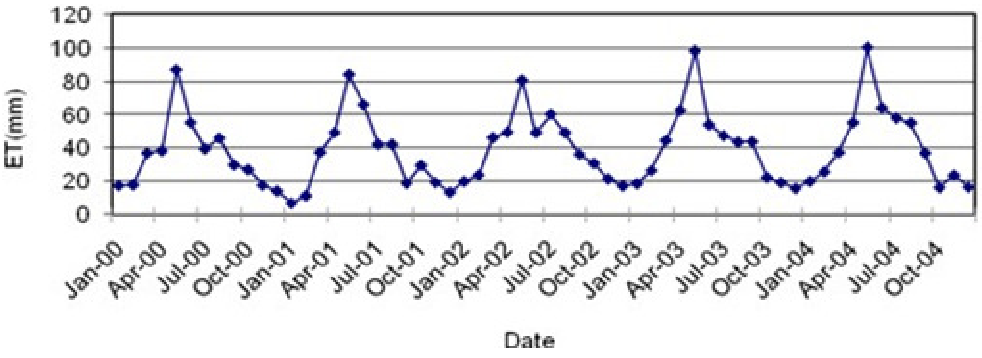

Figure 6. The monthly ET result from the remote sensing based method from the year of 2000 to 2004.

Table 3. Calibrated parameters of the model.

Parameter	Value scope	Value
ESCO	0-1	0.1
SCS runoff curve: CN_2	-8-8	-7
Baseflow a coefficient: ALPHA_BF	0-1	0.041
Soil available water capacity: SOL_AWC	0-1	0.04

Table 4. Estimation of the model simulated result.

Period of time	Re	Ens	R^2
Calibration	0.119	0.875	0.946
Validation	0.101	0.808	0.925

abundant and the temperature is high throughout the year, the ET distribution was uniform in the basin, as shown in Figures 5b and 5c. In December when the temperature was the lowest and the rainfall is the least among the year, as shown in Figure 5, the maximum ET emerged in the upper reaches of the basin and the area with high altitudes, and the total ET was the least among the year due to the low temperature; in this period, the altitude was the major factor affecting the ET distribution in the whole basin.

The seasonal variation of ET was analyzed, as shown in Figure 6. The ET exhibited an obvious rule of seasonal variation, that is, the maximum ET emerged in summer when the temperature is highest and the rainfall is abundant, the ET was less in spring and autumn than in summer, and the ET reached the least throughout the year in winter. In other words, the variation trend of the ET was coordinated with the rainfall and temperature variation in a year.

Runoff simulation with the SWAT model

Due to the regional adaptability, the SWAT model should be calibrated and validated before using. In this study, the data from 2001 to 2004 were adopted for calibration, and the data of 2000 were adopted for validation. According to Nash and Sutcliffe (1970), the model would be evaluated with the following parameters: model efficiency coefficient Ens, mean error Re and correlation coefficient R^2 which was calculated using excel, while Re and Ens were calculated according to the following formula:

$$R_e = \frac{Q_{sim,i} - Q_{obs,i}}{Q_{obs,i}} \times 100\% \quad Ens = 1 - \frac{\sum_{i=1}^{n} \left(Q_{obs,i} - Q_{sim,i}\right)^2}{\sum_{i=1}^{n} \left(Q_{obs,i} - \overline{Q}_{obs}\right)^2} \tag{9}$$

Where, $Q_{obs,i}$ is the observed runoff, $Q_{sim,i}$ is the simulated runoff, and $\overline{Q}_{obs}$ is the average observed runoff.

In the SWAT model, the whole basin was divided into 119 HRUs, as shown in Figure 6. The accepted range after calibration was shown in Table 3.

After the calibration and validation, the evaluation indicators of SWAT were shown in Table 4, with good general performance.

On the basis aforementioned, the data of the monthly simulated runoff using SWAT and the observed data in the Zhelin Basin from 2000 to 2004 were shown in Figure 7.

Comparison of simulated runoff with observed data

For the comparison of the result, we also calculate the runoff with the Penman-Monteith option which embedded in SWAT, as well as the runoff calculation with the remote-sensing retrieval result as the input. The monthly runoff data and the simulated runoff data with SWAT using the two ET methods, especially the remote-sensing retrieval result, in the Zhelin Basin from 2000 to 2004 were shown in comparison in Figure 8.

From the figure and table above, the correlation (R^2=0.8516) between the simulated results based on ET retrieval and the observed data was higher than that (R^2=0.8411) between the results simulated with PM-based ET and the observed data after data fusion. The RMSE (RMSE=26.0860) between the simulated runoff based on ET retrieval and the observed data was obviously smaller than that (RMSE=35.71904) between the runoff simulated with PM-based ET and the observed data. The MBE (MBE=-8.6578) between the simulated runoff based on ET retrieval and the observed data was obviously superior to that (MBE=-22.7313) between the simulated runoff based PM-based ET and the observed data.

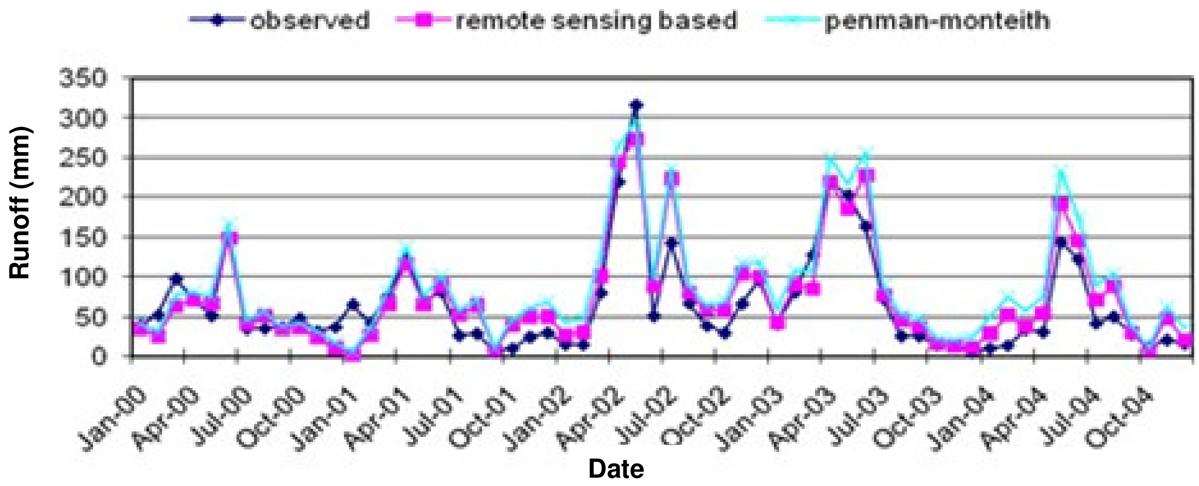

Figure 7. The monthly runoff simulated by SWAT from RS-derived ET, the SWAT embedded penman-monteith ET versus the observed runoff from the year of 2000 to 2004.

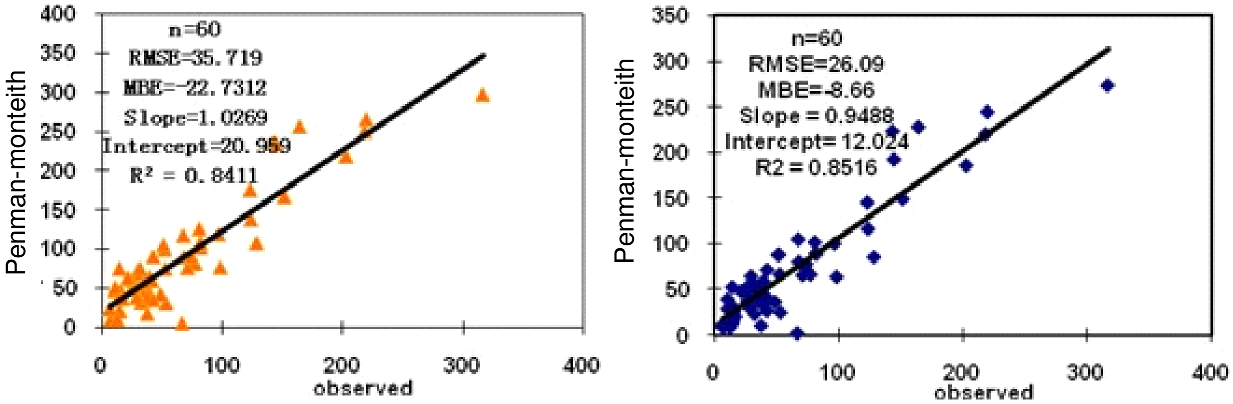

(a) (b)

Figure 8. The monthly runoff simulated from RS-derived ET and Penman-monteith ET with SWAT versus the observed runoff data. (a) The simulated runoff with Penman-monteith model versus the observed runoff; (b) The simulated runoff with remote sensing based model versus the observed runoff.

Currently, it is difficult to validate the retrieval results pixel by pixel directly. However, the underlying conditions of the basin can be taken into account in the distributed hydrological model with high sensitivity to the accuracy of the input data, so that the retrieval results can be validated indirectly through this method and with the support of the distributed hydrological model.

Conclusions

This study presented a new method to validate the ET results from RS retrieval with the support of a distributed hydrological model- the SWAT model. Five years (2000-2004) evapotranspiration data of Zhelin Basin, the study area, were prepared. RS-derived ET and other data (DEM, land-use data, soil data, etc) were processed together in SWAT to simulate the hydrological cycle. The runoff data were then output from the SWAT model. When monthly total runoffs were compared with observed data, the model-estimated data had a RSME of 26.0860 and a R^2 of 0.8516. And the runoff data obtained from RS retrieval of ET was better than those from PM-based ET which was embedded in SWAT in terms of the parameters: RMSE, MBE and R^2. The RS-derived ET was then validated based on the results of comparison.

It indicated that the method presented in the paper was an operational and feasible way for validation of ET data derived from remote sensing data. The subsequent research work of this study should be focused on improving the temporal/spatial resolution of the RS data and enhance the improvement of ET retrieval according to the results of validation.

ACKNOWLEDGEMENTS

This paper was funded by the Earth System Science Data Sharing Program of China (2005DKA32300, http://www.geodata.cn);the National Natural Science Foundation Program of China (40801180、40771146).

REFERENCES

Allen R, Tasumi M, Morse A, Trezza R (2005). A Landsat-based energy balance and evapotranspiration model in Western US water rights regulation and planning. Irrigat. Drain Syst. 19(3):251-268.

Amatya D, Skaggs R, Gregory J (1995). Comparison of methods for estimating REF-ET. J. Irrigat. Drain. Eng. 121(6):427-435.

Arnold J, Srinivasan R, Muttiah R, J Williams (1998). Large area hydrologic modeling and assessment partI: model development1. JAWRA 34(1):73-89.

Arnold. J, Allen P, Bernhardt G (1993). A comprehensive surface-groundwater flow model. J. Hydrol. 142(1-4):47-69.

Bastiaanssen W (2000). SEBAL-based sensible and latent heat fluxes in the irrigated Gediz Basin, Turkey, J. Hydrol. 229(1-2):87-100.

Bastiaanssen W, Menenti M, Feddes R, Holtslag A (1998a). A remote sensing surface energy balance algorithm for land (SEBAL). 1. Formulation. J. Hydrol. 212:198-212.

Bastiaanssen W, Pelgrum H, Wang J, Ma Y, Moreno J, Roerink G, Van der Wal T (1998b). A remote sensing surface energy balance algorithm for land (SEBAL). Part 2: Validation. J. Hydrol. 212:213-229.

Boegh E, Poulsen R, Butts M, Abrahamsen P, Dellwik E, Hansen S, Hasager C, Ibrom A, Loerup J, Pilegaard K (2009). Remote sensing based evapotranspiration and runoff modeling of agricultural, forest and urban flux sites in Denmark: From field to macro-scale. J. Hydrol. 377(3-4):300-316.

Boegh E, Soegaard H, Thomsen A (2002). Evaluating evapotranspiration rates and surface conditions using Landsat TM to estimate atmospheric resistance and surface resistance. Remote. Sens. Environ. 79(2-3):329-343.

Drexler J, Snyder R, Spano D (2004). A review of models and micrometeorological methods used to estimate wetland evapotranspiration. Hydrol. Process. 18(11):2071-2101.

Ficklin D, Luo Y, Luedeling E, Zhang M (2009). Climate change sensitivity assessment of a highly agricultural watershed using SWAT. J. Hydrol. 374(1-2):16-29.

Gao Y (2008). Intercomparison of remote sensing-based models for estimation of evapotranspiration and accuracy assessment based on SWAT. Hydrol. Process. 22(25):4850-4869.

Garcia M, Raes D, Allen R, Herbas C (2004). Dynamics of reference evapotranspiration in the Bolivian highlands (Altiplano). Agric. Forest. Meteorol. 125(1-2):67-82.

Gavilán P, Lorite IJ, Tornero S, Berengena J (2006). Regional calibration of Hargreaves equation for estimating reference ET in a semiarid environment. Agric. Water. Manage. 81(3):257-281.

Granger R (1996). Comparison of surface and satellite-derived estimates of evapotranspiration using a feedback algorithm. Applications of remote sensing in hydrology. pp.71-81.

Granger R (2000). Satellite-derived estimates of evapotranspiration in the Gediz basin. J. Hydrol. 229(1-2):70-76.

Heilman J, McInnes K, Kjelgaard J, Keith Owens M, Schwinning S (2009). Energy balance and water use in a subtropical karst woodland on the Edwards Plateau, Texas. J. Hydrol. 373(3-4):426-435.

Hussey B, Odum W (1992). Evapotranspiration in tidal marshes. Estuar. Coast. 15(1):59-67.

Immerzeel W, Droogers P (2008). Calibration of a distributed hydrological model based on satellite evapotranspiration. J. Hydrol. 349(3-4):411-424.

Jabloun M, Sahli A (2008). Evaluation of FAO-56 methodology for estimating reference evapotranspiration using limited climatic data:: Application to Tunisia. Agric. Water. Manage. 95(6):707-715.

Jacob F, Olioso A, Gu X, Su Z, Seguin B (2002). Mapping surface fluxes using airborne visible, near infrared, thermal infrared remote sensing data and a spatialized surface energy balance model. Agronomie 22(6):669-680.

Jiang D, Wang J (2003). Key hydrologiacal parameters retrieved by using remote sensing technique in the Yellow River Basin. Adv. Water Sci. 14(6):736-739.

Kannan N, White S, Worrall F, Whelan M (2007a). Sensitivity analysis and identification of the best evapotranspiration and runoff options for hydrological modelling in SWAT-2000. J. Hydrol. 332(3-4):456-466.

Kannan N, White S, Worrall F, Whelan M (2007b). Hydrological modelling of a small catchment using SWAT-2000-Ensuring correct flow partitioning for contaminant modelling. J. Hydrol. 334(1-2):64-72.

Kite G, Droogers P (2000). Comparing evapotranspiration estimates from satellites, hydrological models and field data J. Hydrol. 229(1-2):3-18.

Kustas W, Moran M, Humes K, Stannard D, Pinter P Jr, Hipps L, Swiatek E, Goodrich D (1994). Surface energy balance estimates at local and regional scales using optical remote sensing from an aircraft platform and atmospheric data collected over semiarid rangelands. Water Resour. Res. 30(5):1241-1259.

Kustas W, Norman J (1999). Evaluation of soil and vegetation heat flux predictions using a simple two-source model with radiometric temperatures for partial canopy cover. Agric. Forest. Meteorol. 94(1):13-29.

Liu R, Wen J, Wang X, Wang L, Tian H, Zhang T, Shi X, Zhang J, Lv S (2010). Actual daily evapotranspiration estimated from MERIS and AATSR data over the Chinese Loess Plateau. Hydrol. Earth. Syst. Sc. 14:47-58.

Lopez-Urrea R, Martin de Santa Olalla F, Fabeiro C, Moratalla A (2006). Testing evapotranspiration equations using lysimeter observations in a semiarid climate. Agric. Water. Manage. 85(1-2):15-26.

Mohan S (1991). Intercomparison of evapotranspiration estimates. Hydrolog. Sci. J. 36(5):447-460.

Monteith J (1973). Principles of environmental physics, Edward Arnold. London. P. 241.

Moran M, Kustas W, Vidal A, Stannard D, Blanford J, Nichols W (1994). Use of ground-based remotely sensed data for surface energy balance evaluation of a semiarid rangeland. Water. Resour. Res. 30(5):1339-1349.

Nash J, Sutcliffe J (1970). River flow forecasting through conceptual models part I--A discussion of principles. J. Hydrol. 10(3):282-290.

Neitsch S, Arnold J, Kiniry J, Williams J, King K (2001). Soil and Water Assessment Tool-Version 2000-User's Manual, Temple, Texas.

Neitsch S, Arnold J, Kiniry J, Williams J, King K (2002). Soil and water assessment tool theoretical documentation version 2000, Grassland. Soil Water Research Laboratory Temple Texas.

Overgaard J, Rosbjerg D, Butts M (2006). Land-surface modelling in hydrological perspective: a review. Biogeosciences 3(2):229-241.

Parasuraman K, Elshorbagy A, Carey S (2007). Modelling the dynamics of the evapotranspiration process using genetic programming. Hydrolog. Sci. J. 52(3):563-578.

Sun L, Song C (2008). Evapotranspiration from a freshwater marsh in the Sanjiang Plain, Northeast China. J. Hydrol. 352(1-2):202-210.

Wang J, Jiang D (2005). Study on the duality water circulation of the Yellow river basin.

Wu W, Hall C, Scatena F, Quackenbush L (2006). Spatial modelling of evapotranspiration in the Luquillo experimental forest of Puerto Rico using remotely-sensed data. J. Hydrol. 328(3-4):733-752.

Zhang B, Kang S, Li F, Zhang L (2008). Comparison of three evapotranspiration models to Bowen ratio-energy balance method for a vineyard in an arid desert region of northwest China. Agric. Forest. Meteorol. 148(10):1629-1640.

Zhou L, Zhou G (2009). Measurement and modelling of evapotranspiration over a reed (Phragmites australis) marsh in Northeast China. J. Hydrol. 372(1-4):41-47.